ISSN 1070-3284, Russian Journal of Coordination Chemistry, 2015, Vol. 41, No. 7, pp. 428–435. © Pleiades Publishing, Ltd., 2015.
Original Russian Text © A.V. Piskunov, M.G. Chegerev, L.B. Vaganova, G.K. Fukin, 2015, published in Koordinatsionnaya Khimiya, 2015, Vol. 41, No. 7, pp. 394–402.

New Paramagnetic Tin(IV) Complexes Based on *o*-Iminoquinone Ligands: Synthesis and Thermal Transformation

A. V. Piskunov[a, b, *], M. G. Chegerev[a, b], L. B. Vaganova[b], and G. K. Fukin[a, b]

[a] *Razuvaev Institute of Organometallic Chemistry, Russian Academy of Sciences, ul. Tropinina 49, Nizhni Novgorod, 603600 Russia*

[b] *Nizhni Novgorod State University, pr. Gagarina 23, Nizhni Novgorod, 603600 Russia*

**e-mail: pial@iomc.ras.ru*

Received December 15, 2014

Abstract—A series of new paramagnetic tin(IV) complexes based on sterically hindered *o*-iminobenzoquinones (R)ImQ differed in fragments (R) in the N-aryl fragment is synthesized. The thermal transformation of the tin(IV) complex, (*iso*-Pr)ImSQSn(*tert*-Bu)$_2$Cl ((*iso*-Pr)ImSQ is the radical anion of 4,6-di-*tert*-butyl-N-(2,6-di-*iso*-propylphenyl)-*o*-iminobenzoquinone), is studied. The thermal transformation of the paramagnetic complex in nonane results in the formation of a new tin(II) bis(aminophenolate) derivative. The synthesized complexes and the thermolysis product are characterized by EPR, IR, and ^{1}H, ^{13}C, and ^{119}Sn NMR spectroscopy and elemental analysis. The structures of the (*tert*-Bu)ImSQSn(*tert*-Bu)$_2$Cl complex and the thermal decomposition product, {(*iso*-Pr)AmPh}$_2$Sn ((*iso*-Pr)AmPh is 2-(2,6-di-*iso*-propylphenyl)amino-4,6-di-*tert*-butylphenolate), are determined by X-ray diffraction analysis.

DOI: 10.1134/S1070328415070076

INTRODUCTION

The study of chemical redox transformations is an urgent trend of the chemistry of coordination compounds, because the most part of chemical and biochemical processes is classified as redox reactions. A promising direction in this field is the study of the chemistry of metal complexes with redox-active ligands capable of staged oxidizing or reducing in the coordinated state under the action of external agents. This property determines the appearance of unusual chemical properties of similar compounds, in particular, the easy occurrence of redox transformations. The nontransition metal complexes of this type are of special interest. The introduction of a redox-active ligand into the coordination sphere of the main subgroup metal makes it possible to substantially extend the range of reduction and oxidation possibilities of compounds of this metal, since they are not characterized by many oxidation states, unlike transition metals. The appearance of this property allows one to use similar complexes in reactions of oxidative addition and reductive elimination, where the redox-active ligand is subjected to oxidation and reduction rather than the metal center. Thus, the complex formation of redox-active ligands with nontransition metals makes it possible to imitate the behavior of the transition metal complexes. The reversible addition of oxygen to the antimony catecholate and amidophenolate complexes [1–5] and the fixation of nitrogen monoxide by the lead and zinc catecholate complexes [6] were carried out. The gallium and aluminum complexes with the redox-active diiminoacenaphthene ligand (BIAN) capable of activating the C≡C triple bond in alkynes were reported [7, 8]. The possibility of haloid alkyl activation by the indium [9], gallium [10], and tin [11] *o*-amidophenolate complexes was also shown. In these complexes, the redox state of the redox-active ligand changes, but the central atom does not change its state.

Nontransition metal complexes with redox-active ligands have recently found use in the chemistry of macromolecules, namely, in controlled radical polymerization [12–18]. At present, these processes mainly involve transition metal complexes. However, as we have shown previously [12–16], the introduction of the tin catecholate complexes into a polymerizing system makes it possible to control the polymer chain growth by the reversible addition and elimination of growing radicals by these complexes. The introduction of paramagnetic tin *o*-iminosemiquinolate complexes, (*iso*-Pr)ImSQSnR$_2$Cl ((*iso*-Pr)ImSQ is the 4,6-di-*tert*-butyl-N-(2,6-di-*iso*-propylphenyl)-*o*-iminobenzoquinone, R = Me, Et, *tert*-Bu, Ph, and Cl), [17] allows one to carry out the synthesis of poly(methyl methacrylate) without a gel effect. The numerical mean molecular weight of the polymer increases linearly with an increase in the conversion, and the polydispersity of the poly(methyl methacrylate) samples decreases. The tin complex of the (*iso*-Pr)ImSQSn(*tert*-Bu)$_2$Cl type is of special interest,

since this complex exhibits the properties of an iniferter, i.e., acts as both an initiator of methyl methacrylate polymerization and a regulator of the polymer chain growth. This fact is likely explained by the high initiating ability of the *tert*-Bu radical formed in the system upon the thermal decomposition of the initial complex. The formation of the *tert*-Bu radical is due to the homolysis of the labile Sn–*tert*-Bu bond having the lowest metal–carbon bond energy among the alkyl and aryl tin derivatives. The thermal decomposition of (*iso*-Pr)ImSQSn(*tert*-Bu)$_2$Cl occurs when the reaction system is heated to 70–90°C (polymerization temperature)[18].

This work is devoted to the synthesis of new tin(IV) complexes with the redox-active *o*-iminoquinone ligands differed in substituents in the N-phenyl fragment and to the study of the thermal transformation of {(*iso*-Pr)ImSQ}Sn(*tert*-Bu)$_2$Cl. It is urgent to establish the possible route and products of the thermal decomposition of the considered complex because makes it possible to determine the mechanism of the work of organometallic iniferters of a similar type.

EXPERIMENTAL

Experiments on the synthesis and study of the tin(IV) *o*-iminobenzoquinone complexes were carried out under reduced pressure in the presence of traces of oxygen and air moisture.

IR spectra were recorded on an FSM-1201 FT-IR spectrometer in Nujol using KBr cells. EPR spectra were detected on a Bruker EMX spectrometer. 2,2-Diphenyl-1-picrylhydrazyl ($g = 2.0037$) was used as a standard for the determination of the *g* factor. The EPR spectra were simulated using the WinEPR SimFonia program (Bruker) to determine the exact parameters. NMR spectra were recorded in a C_6D_6 solution on a Bruker Avance III instrument (400 MHz) using tetramethylsilane as an internal standard. The precise assignment of signals in the NMR spectra was performed using the 2D ge-COSY and ge-HSQC procedures.

The solvents used were purified and dehydrated according to published recommendations [19].

Disodium salts of various *o*-iminoquinones (R)APNa$_2$ were synthesized by the direct reduction of (R)ImQ with a sodium excess in tetrahydrofuran (THF). The color of the reaction solution changed from vinous red to bright yellow.

Monosodium salts (R)ImSQNa were synthesized by the reactions of sodium *o*-amidophenolates (R)APNa$_2$ with the corresponding *o*-iminoquinones in a molar ratio of 1 : 1 in THF. The reactions were accompanied by a change in the color of the solution from bright yellow to blue. Compound (R)ImSQNa was used in the in situ syntheses.

Syntheses of the complexes (I–IV). A solution of sodium *o*-iminosemiquinolate (R)ImSQNa (1.0 mmol) in THF (20 mL) was slowly poured to a solution of tin(IV) di-*tert*-butyl dichloride (1.0 mmol) in THF (10 mL): the color of the reaction mixture changed from blue to brown. The obtained solution was stirred at room temperature for 15 min, and the solvent was removed under reduced pressure. The residue was treated with hexane (40 mL) and filtered on the Schott glass filter no. 4. The hexane solution was evaporated to half a volume and slowly cooled to –18°C. The formed crystals of the tin *o*-iminosemiquinone complexes were decanted from the mother liquor and dried under reduced pressure.

[4,6-Di-*tert*-butyl-N-(2,6-dimethylphenyl)-*o*-iminobenzosemiquinolato]di-*tert*-butylchlorotin(IV) (**I**): the yield of the analytically pure product was 0.50 g (85%).

For $C_{30}H_{47}NOClSn$

anal. calcd., %: C, 60.88; H, 8.00; Cl, 5.99; Sn, 20.06.

Found, %: C, 60.83; H, 8.14; Cl, 5.90; Sn, 20.09.

IR (ν, cm^{-1}): 1583, 1439, 1360, 1332, 1317, 1264, 1247, 1200, 1199, 1159, 1113, 1098, 1101, 1032, 1013, 954, 936, 912, 874, 860, 822, 804, 774, 738, 660, 648, 627, 607, 631, 537, 491.

[4,6-Di-*tert*-butyl-N-(2-ethyl-6-methyl)-*o*-iminobenzosemiquinolato]di-*tert*-butylchlorotin(IV) (**II**): the yield of the analytically pure product was 0.47 g (78%).

For $C_{31}H_{49}NOClSn$

anal. calcd., %: C, 61.45; H, 8.15; Cl, 5.85; Sn, 19.59.

Found, %: C, 61.43; H, 8.10; Cl, 5.80; Sn, 19.50.

IR (ν, cm^{-1}): 1586, 1438, 1389, 1365, 1334, 1251, 1198, 1161, 1113, 1103, 1028, 1015, 993, 937, 914, 895, 875, 865, 823, 803, 778, 740, 657, 649, 627, 605, 578, 530, 496.

[4,6-Di-*tert*-butyl-N-(2,6-diethylphenyl)-*o*-iminobenzosemiquinolato]di-*tert*-butylchlorotin(IV) (**III**): the yield of the analytically pure product was 0.49 g (80%).

For $C_{32}H_{51}NOClSn$

anal. calcd., %: C, 62.00; H, 8.29; Cl, 5.72; Sn, 19.15.

Found, %: C, 62.13; H, 8.24; Cl, 5.70; Sn, 19.09.

IR (ν, cm^{-1}): 1587, 1452, 1392, 1364, 1333, 1252, 1199, 1160, 1115, 1058, 1031, 1015, 1032, 1013, 992, 939, 913, 875, 826, 805, 804, 773, 712, 660, 650, 628, 605, 564, 529, 496.

[4,6-Di-*tert*-butyl-N-(2,5-di-*tert*-butylphenyl)-*o*-iminobenzosemiquinolato]di-*tert*-butylchlorotin(IV) (**IV**):

the yield of the analytically pure product was 0.58 g (86%).

For $C_{36}H_{59}NOClSn$

anal. calcd., %: C, 63.96; H, 8.80; Cl, 5.24; Sn, 17.56.

Found, %: C, 64.05; H, 8.90; Cl, 5.20; Sn, 17.47.

IR (ν, cm^{-1}): 1579, 1552, 1498, 1435, 1392, 1365, 1332, 1296, 1269, 1250, 1200, 1158, 1133, 1109, 1070, 1033, 1017, 997, 1013, 902, 885, 895, 862, 842, 822, 804, 777, 744, 722, 688, 656, 620, 602, 544, 525, 497.

Thermal decomposition of (*iso*-Pr)ImSQSn(*tert*-Bu)$_2$Cl (V). A weighed sample of compound **V** (0.5 g) was dissolved in nonane (20 mL). The obtained solution was heated in a boiling water bath for a week: the color of the reaction mixture changed from brown to yellow. After the end of the reaction, the solution was evaporated to half a volume and kept at room temperature. The isolated crystalline product {(*iso*-Pr)AmPh}$_2$Sn (**VI**) was characterized by NMR and IR spectroscopy and X-ray diffraction analysis.

Bis(2-(2,6-di-*iso*-propylphenyl)amino-4,6-di-*tert*-butylphenolato)tin(II) (**VI**): the yield of the analytically pure product was 0.13 g (80%).

For $C_{52}H_{76}N_2O_2Sn$

anal. calcd., %: C, 70.98; H, 8.71; O, 3.64; Sn, 13.49.

Found, %: C, 71.10; H, 8.65; O, 3.74; Sn, 13.54.

^{1}H NMR (δ, ppm): 1.05 (br.s, 12 H, 4 CH_3(*iso*-Pr)), 1.17 (s, 18 H, 6 CH_3(*tert*-Bu)), 1.28 (br.s, 12 H, 4 CH_3(*iso*-Pr)), 1.53 (s, 18 H, 6 CH_3(*tert*-Bu)), 3.45 (br.s, 4 H(*iso*-Pr)), 6.65 (s, 2 H(NH), $J_{^{119}Sn-H}$ = 16.4 Hz), 6.81 (d, 2 H, $CH_{aminophenol}$, J_{H-H} = 2.2 Hz, $J_{^{119}Sn-H}$ = 8.8 Hz), 7.04–7.16 (m, 6 H, $CH_{aniline}$), 7.28 (d, 2 H, $CH_{aminophenol}$, J_{H-H} = 2.2 Hz). ^{13}C NMR (δ, ppm): 23.52 ($\underline{C}H_3$(*iso*-Pr)), 24.72 ($\underline{C}H_3$(*iso*-Pr)), 28.41 ($\underline{C}$(*iso*-Pr)), 29.48 ($\underline{C}H_3$(*tert*-Bu)), 31.40 ($\underline{C}H_3$(*tert*-Bu)), 33.82 ($\underline{C}$(*tert*-Bu)), 35.21 ($\underline{C}$(*tert*-Bu)), 120.41 ($\underline{C}H_{aminophenol}$), 121.60 ($\underline{C}H_{aminophenol}$), 125.74, 127.40, 127.70, 127.97, 134.06, 138.09, 138.25, 139.08, 141.26 ($\underline{C}_{aniline+aminophenol}$), 156.86 ($\underline{C}$–$O_{aminophenol}$). ^{119}Sn (δ, ppm): –295.19.

IR (ν, cm^{-1}): 3296, 3284, 1604, 1594, 1563, 1414, 1362, 1351, 1338, 1302, 1258, 1244, 1206, 1183, 1162, 1122, 1103, 1056, 1043, 998, 965, 945, 915, 901, 890, 863, 834, 818, 794, 767, 760, 742, 693, 659, 649, 574, 564, 540, 528, 503, 480, 468.

The X-ray diffraction analyses for compounds IV and VI. Single crystals suitable for X-ray diffraction analysis were obtained from *n*-hexane and *n*-nonane, respectively. The X-ray diffraction analyses were carried out on a Smart Apex I diffractometer (MoK_α radiation, graphite monochromator) at 100(2) K. The structures of compounds **IV** and **VI** were solved by a direct method followed by the refinement using full-matrix least squares for F^2 (SHELXTL) [20]. An absorption correction was applied using the SADABS program [21]. All non-hydrogen atoms were refined in the anisotropic approximation. Hydrogen atoms were placed in the geometrically calculated positions and refined in the riding model. The crystallographic data and the main refinement parameters for structures **IV** and **VI** are presented in Table 1. Selected bond lengths and angles are listed in Table 2.

The crystallographic data for the studied complexes were deposited with the Cambridge Crystallographic Data Centre (CCDC 1034817 (**IV**) and 1034818 (**VI**); deposit@ccdc.cam.ac.uk or http://www.ccdc.cam.ac.uk/data_request/cif).

RESULTS AND DISCUSSION

Exchange reactions between alkaline metal derivatives and metal halides are widely used for the synthesis of diverse coordination compounds. The reaction of (R)ImSQNa with tin di-*tert*-butyl dichloride in a THF solution occurs very easily, ceases for 15 min at room temperature, and is accompanied by a change in the color of the reaction mixture from blue to brown. The brown color is characteristic of the radical anion form of the *o*-iminosemiquinone ligand in the tin(IV) complexes (Scheme 1).

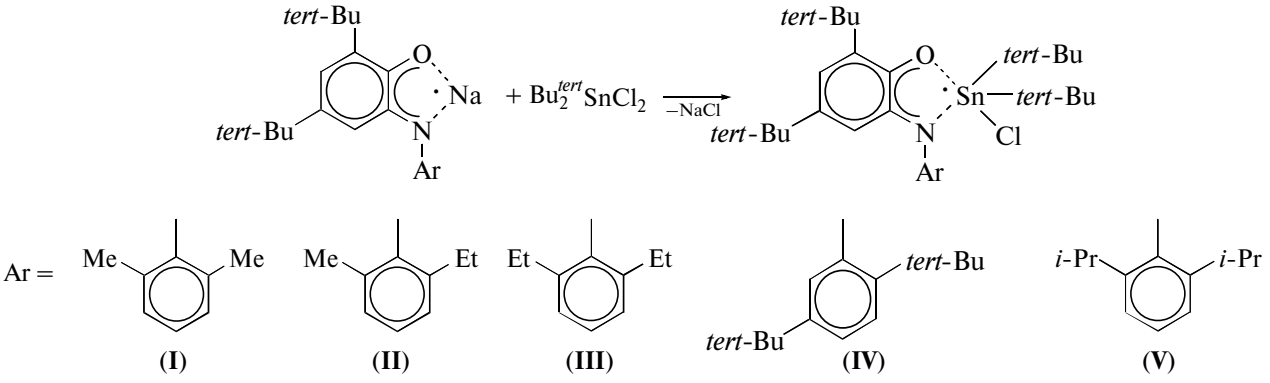

Scheme 1.

Table 1. Crystallographic data and the X-ray diffraction experimental and refinement parameters for complexes **IV** and **VI**

Parameter	Value	
	IV	**VI**
FW	675.98	879.84
Crystal system	Monoclinic	Triclinic
Space group	$P2_1/n$	$P\bar{1}$
a, Å	10.9837(6)	10.9961(3)
b, Å	15.3486(9)	15.3638(4)
c, Å	21.7499(13)	16.7419(4)
α, deg	90	64.66
β, deg	102.6510(10)	88.4820(10)
γ, deg	90	76.3580(10)
V, Å^3	3577.7(4)	2475.23(11)
Z	4	2
F(000)	1428	936
ρ_{calcd}, g/cm^3	1.255	1.180
μ, mm^{-1}	0.815	0.554
Crystal size, mm	0.23 × 0.18 × 0.15	0.41 × 0.23 × 0.19
Measurement θ range, deg	1.92–25.00	1.91–26.00
Ranges of reflection indices	$-13 \le h \le 13$, $-18 \le k \le 18$, $-25 \le l \le 25$	$-13 \le h \le 13$, $-18 \le k \le 18$, $-20 \le l \le 20$
Number of observed reflections	28101	21421
Number of independent reflections	6284	9659
R_{int}	0.0341	0.0166
Goodness-of-fit (F^2)	1.005	1.068
R_1, wR_2 ($I > 2\sigma$, I)	0.0380, 0.0929	0.0252, 0.0649
R_1, wR_2 (for all reflections)	0.0468, 0.0968	0.0273, 0.0660
Residual electron density (max/min), *e* Å^{-3}	2.743/–0.366	0.849/–0.670

Crystallization from hexane solutions gave dark brown products **I**–**IV**. Complex **V** was obtained using a known procedure [22]. All obtained tin *o*-iminosemiquinone complexes in the crystalline state are resistant to air oxygen and moisture. They are paramagnetic in both the crystalline state and solution and are characterized by well resolved EPR spectra (Fig. 1).

The EPR spectrum of complex **IV** represents a triplet (1 : 1 : 1) of doublets (1 : 1). The hyperfine structure of the spectrum is caused by the interaction of a unpaired electron with the magnetic nuclei of the ^{1}H hydrogen atom (99.98%, $I = 1/2$, $\mu_N = 2.7928$) [23] and ^{14}N nitrogen atom (99.63%, $I = 1$, $\mu_N = 0.4037$) [23]. In addition, a satellite splitting on the magnetic tin isotopes ^{117}Sn (7.68%, $I = 1/2$, $\mu_N = 1.000$) and ^{119}Sn (8.58%, $I = 1/2$, $\mu_N = 1.046$) is observed [23]. The shapes of the spectra of compounds **I**–**III** are similar to that of complex **IV**, and the values of hyperfine coupling constants and *g* factors are given in Table 3.

Since the EPR spectrum of compound **IV** contains no hyperfine coupling of the unpaired electron with the magnetic isotopes ^{35}Cl and ^{37}Cl, it can be assumed that the halogen atom is closely localized to the plane of the *o*-iminosemiquinolate ligand. This assumption is consistent with the X-ray diffraction analysis data (Fig. 2).

The coordination polyhedron of the tin atom in compound **IV** is a distorted trigonal bipyramid. The O(1) oxygen atom of the *o*-iminosemiquinone ligand and the Cl(1) atom occupy the apical positions. The equatorial plane of the bipyramid is formed by the N(1) nitrogen atoms and the C(29) and C(33) carbon atoms of the alkyl substituents at the tin atom. According to the radical anion state, the characteristic distribution of bond lengths in the *o*-iminoquinone ligand of complex **IV** is observed [22]. The C(1)–O(1) (1.304(3) Å) and C(2)–N(1) (1.345(3) Å) distances lie in the range characteristic of the *o*-iminosemiquinone metal complexes [22]. The six-membered ring C(1)–C(6) in molecule **IV** demonstrates a quinoid type of distortion characteristic of *o*-iminosemiquinones manifested as an alternation of the C–C bond lengths. The C(1)–C(2), C(1)–C(6), C(2)–C(3), and

Table 2. Selected bond lengths (Å) and angles (deg) in complexes **IV** and **VI**

Bond	*d*, Å	Bond	*d*, Å
		IV	
Sn(1)–N(1)	2.177(2)	N(1)–C(15)	1.452(3)
Sn(1)–O(1)	2.2017(17)	C(1)–C(6)	1.441(3)
Sn(1)–Cl(1)	2.4537(6)	C(1)–C(2)	1.441(3)
Sn(1)–C(29)	2.205(3)	C(2)–C(3)	1.417(4)
Sn(1)–C(33)	2.190(3)	C(3)–C(4)	1.368(4)
O(1)–C(1)	1.304(3)	C(4)–C(5)	1.436(4)
N(1)–C(2)	1.345(3)	C(5)–C(6)	1.377(4)
		VI	
Sn(1)–O(1)	2.0958(8)	C(2)–C(3)	1.3899(18)
Sn(1)–O(2)	2.0798(8)	C(3)–C(4)	1.3892(18)
Sn(1)–N(2)	2.4315(11)	C(4)–C(5)	1.4036(18)
Sn(1)–N(1)	2.4585(11)	C(5)–C(6)	1.3921(18)
O(1)–C(1)	1.3431(15)	C(27)–C(32)	1.4152(16)
O(2)–C(27)	1.3486(16)	C(28)–C(29)	1.3838(19)
N(1)–C(15)	1.4512(16)	C(29)–C(30)	1.3880(17)
N(1)–C(2)	1.4584(15)	C(30)–C(31)	1.3980(18)
N(2)–C(28)	1.4655(14)	C(30)–C(33)	1.5375(19)
C(1)–C(2)	1.4029(18)	C(31)–C(32)	1.3951(19)
C(1)–C(6)	1.4214(17)		
Angle	ω, deg	Angle	ω, deg
		IV	
N(1)Sn(1)C(33)	105.58(9)	C(1)O(1)Sn(1)	116.17(15)
N(1)Sn(1)O(1)	73.62(7)	C(2)N(1)Sn(1)	116.53(16)
N(1)Sn(1)C(29)	131.30(9)	C(2)N(1)C(15)	118.1(2)
C(33)Sn(1)C(29)	121.23(10)	C(33)Sn(1)C(29)	121.23(10)
N(1)Sn(1)Cl(1)	87.44(6)	O(1)Sn(1)C(29)	87.79(8)
O(1)Sn(1)Cl(1)	156.99(5)	C(33)Sn(1)O(1)	96.38(8)
		VI	
O(2)Sn(1)O(1)	91.04(3)	C(1)O(1)Sn(1)	122.17(8)
O(2)Sn(1)N(2)	75.07(3)	C(27)O(2)Sn(1)	119.50(7)
O(1)Sn(1)N(2)	72.67(4)	C(2)N(1)Sn(1)	107.50(7)
O(2)Sn(1)N(1)	78.61(3)	C(28)N(2)Sn(1)	105.24(7)
O(1)Sn(1)N(1)	73.36(3)	C(29)C(28)N(2)	119.82(11)
N(2)Sn(1)N(1)	136.11(3)	C(27)C(28)N(2)	117.54(11)

Table 3. Parameters of the EPR spectra of complexes **I**–**III**

Complex	$a_i(^1H)$, Oe	$a_i(^{14}N)$, Oe	$a_i(^{117}Sn,^{119}Sn)$, Oe	g_i
I	4.1	7.0	48.6; 50.9	2.0029
II	4.1	7.0	48.5; 50.7	2.0029
III	4.2	7.1	48.2; 50.4	2.0029

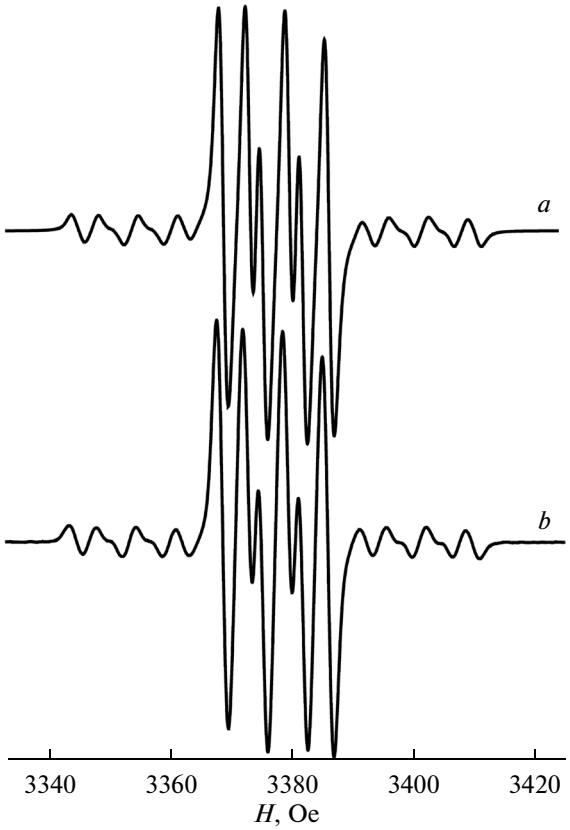

Fig. 1. Isotropic EPR spectra of complex **IV**: (*a*) simulated and (*b*) experimental spectra in THF at $T = 298$ K. Parameters of the EPR spectrum: $a_i(H) = 4.3$ Oe, $a_i(N) = 7.5$ Oe, $a_i(^{117}Sn) = 46.5$ Oe, and $a_i(^{119}Sn) = 48.6$ Oe; $g_i = 2.0028$.

C(4)–C(5) (1.417(4)–1.441(3) Å) distances are much longer than C(3)–C(4) and C(5)–C(6) (1.368(4) and 1.377(4) Å). The chelating *o*-iminosemiquinone ligand is nearly planar: the Cl(1) atom deviates from the plane by 0.317 Å. The Sn(1)–O(1) (2.2017(17) Å) and Sn(1)–N(1) (2.177(2) Å) bond lengths are more than the sum of the covalent radii of the Sn and O (2.11 Å) and Sn and N (2.16 Å) atoms [24], respectively, but are less than the sum of the van der Waals radii of the same atoms (3.7 Å in the case of Sn and O and 3.8 Å for Sn and N [24]), which is also characteristic of the chelate binding of the *o*-iminosemiquinone ligand with the metal center.

The quantitative thermolysis of complex **V** in nonane was carried out to study a possible route of the thermal decomposition of the tin *o*-iminosemiquinone complexes. After the end of thermal decomposition, the EPR signal belonging to the initial paramagnetic compound disappears and a white crystalline substance precipitates from the reaction mixture. According to the X-ray diffraction analysis data, the isolated crystals represent bis(2-(2,6-di-*iso*-propylphenyl)amino-4,6-di-*tert*-butylphenolato)tin(II) (**VI**). The coordination polyhedron of the tin atom in compound **VI**

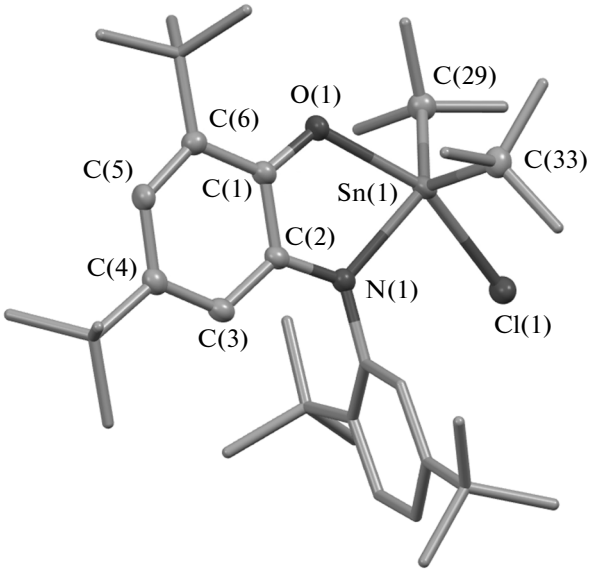

Fig. 2. Molecular structure of complex **IV** (thermal ellipsoids of 50% probability). Hydrogen atoms are omitted.

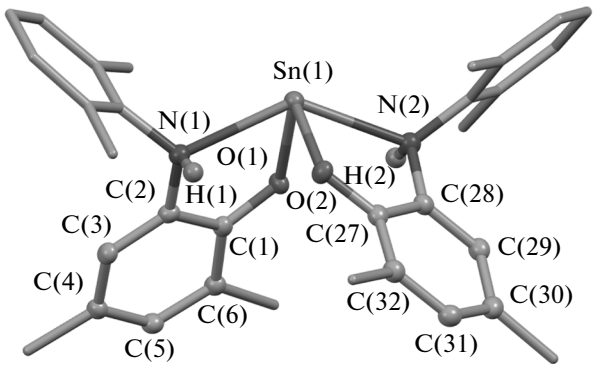

Fig. 3. Molecular structure of complex **IV** (thermal ellipsoids of 50% probability). The methyl groups of the *iso*-propyl and *tert*-butyl groups and hydrogen atoms, except for H(1) and H(2), are omitted for clarity.

is a distorted tetragonal pyramid (Fig. 3), whose equatorial plane is formed by the O(1), O(2) and N(1), N(2) atoms of two ligands. The apical position of the pyramid is occupied by the lone electron pair of the divalent tin atom. The C(1)–O(1) (1.304(3) Å) and C(2)–N(1) (1.345(3) Å) distances are in the range characteristic of ordinary C–O and C–N bonds. The Sn(1)–O(1) (2.0958(8) Å) and Sn(1)–O(2) (2.0798(8) Å) bond lengths are slightly (on the average, by 0.02 Å) less than the sum of the covalent radii of the Sn and O atoms, indicating the covalent binding between the tin atom and oxygen atoms. The Sn(1)–N(1) (2.4585(11) Å) and Sn(1)–N(2) (2.4315(11) Å) distances are by 0.24 Å (on the average) longer than

the sum of the covalent radii of these atoms but are considerably shorter than the sum of the van der Waals radii of the Sn and N atoms, which indicates the donor–acceptor nature of these bonds. All bond lengths in the C(1)–C(6) and C(27)–C(32) rings in both *o*-aminophenolate fragments are close to those in benzene (1.40 Å). The dihedral angle between the planes of two aminophenolate ligands is 73°. Such a small angle is due to the lone electron pair at the tin atom that occupies a space in the coordination sphere of the metal. The distances between the atoms H(1)–O(2) (2.46 Å) and H(2)–O(1) (2.27 Å) are substantially shorter than the sum of the van der Waals radii of the oxygen and hydrogen atoms (2.7 Å) [24], which allows us to assert that the hydrogen atom of the NH group and the oxygen atom of the adjacent aminophenolate ligand are linked by an intramolecular hydrogen bond. Probably, this interaction contributes to a decrease in the dihedral angle between the planes of the ligands.

The ^{119}Sn NMR spectrum exhibits a signal (–295.19 ppm) characteristic of the tetracoordinated tin(II) compounds [25]. The signals from the methine protons and methyl groups of the *iso*-propyl substituents in the ^{1}H NMR spectrum of complex **VI** at room temperature appear as broadened singlets. However, the signals from these groups are well resolved with an increase in temperature. For example, as the temperature increases to 50°C, the broadened singlet from the methine protons at 3.45 ppm is transformed into a septet caused by the splitting on protons of two methyl groups. The broadened singlets from the methyl groups (1.05 and 1.28 ppm) caused by the splitting of the methyl protons on the methine ones are transformed into well resolved doublets. This fact indicates that dynamic processes occur in a solution of compound **VI**.

The IR spectrum of compound **VI** is characterized by a large set of lines. The doublet at 3296 and 3284 cm^{-1} corresponding to the stretching vibrations of the N–H bonds should be mentioned. The presence of this doublet assumes that the Sn(1)–N(1) and Sn(1)–N(2) coordination bonds in the complex are not equivalent, most likely, because of the dynamics of the alternative coordination and decoordination of the nitrogen atoms to the metal. These transformations occur in solution very easily and rapidly, which is confirmed by the presence of only one singlet from the proton of the N–H group in the ^{1}H NMR spectrum. The dynamics of the coordination sphere of a similar type for the low-valence derivatives of the 14 Group elements with the nitrogen-containing neutral ligands is well known [26].

The studies of the thermal decomposition of compound **IV** in nonane at 90°C show that the decrease in the concentration of the paramagnetic compound obeys the kinetic equation of the second order [18]. Using this fact, literature data on the thermal transformation of the tin *o*-semiquinone complexes [27], and the data on the thermal decomposition products, we can propose the most probable mechanism of the transformation. At the first stage, the interaction of two molecules of compound **IV** involves the concerted transfer of the *tert*-butyl radical from one molecule to another to form *o*-amidophenolatochlorotin (a) and the stannoxyl derivative (b) (Scheme 2).

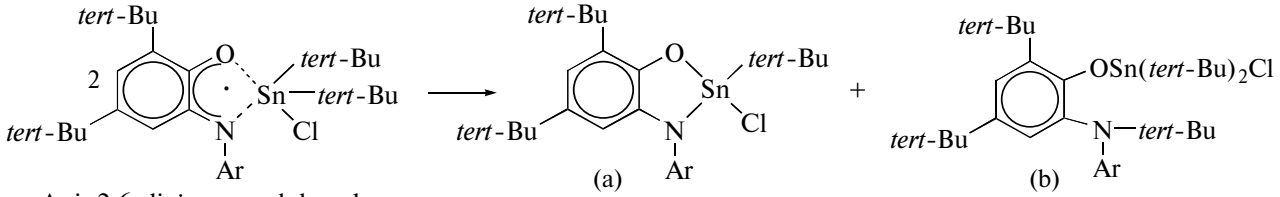

Ar is 2,6-di-*iso*-propylphenyl

Scheme 2.

At the next stage, two molecules (a) are dimerized through the bridging chlorine atoms to form the product (b). The further transformation is related to the ejection of two isobutylene molecules detected by the GC/MS method when analyzing the gas phase and to the formation of tin dichloride. The final product of thermal decomposition is low-valence tin derivative **VI** (Scheme 3).

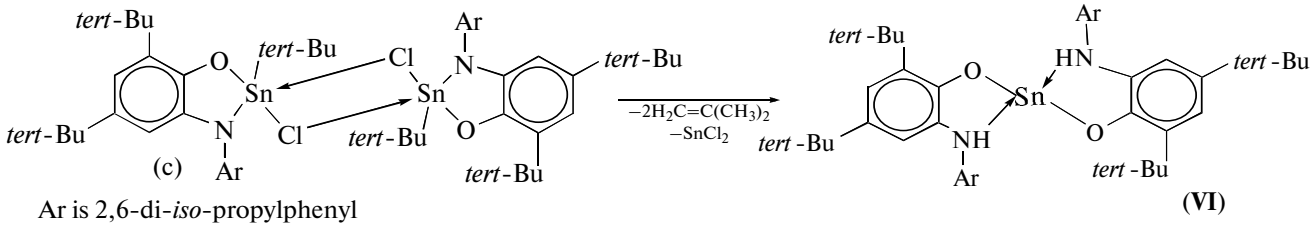

Ar is 2,6-di-*iso*-propylphenyl

Scheme 3.

Thus, we showed that the thermal transformation of the paramagnetic tin(IV) complex based on sterically hindered 4,6-di-*tert*-butyl-N-(2,6-di-*iso*-propylphenyl)-*o*-iminobenzoquinone, {(*iso*-Pr)ImSQ}Sn(*tert*-Bu)$_2$Cl (**V**), was accompanied by a cascade of consecutive reactions leading to the formation of the new tetracoordinated tin(II) bis(aminophenolate) derivative.

ACKNOWLEDGMENTS

This work was supported by the Russian Foundation for Basic Research (project no. 14-03-31032-mol_a), the Council at the President of the Russian Federation for support of leading scientific schools (NSh-271.2014.3), and the Foundation for competitive support of students, postgraduates, and young scientific and pedagogical workers of the Nizhni Novgorod State University.

REFERENCES

1. Abakumov, G.A., Poddel'sky, A.I., Grunova, E.V., et al., *Angew. Chem., Int. Ed. Engl.*, 2005, vol. 44, no. 18, p. 2767.
2. Cherkasov, V.K., Abakumov, G.A., Grunova, E.V., et al., *Chem.-Eur. J.*, 2006, vol. 12, no. 14, p. 3916.
3. Poddel'sky, A.I., Kuskii, Y.A., Piskunov, A.V., et al., *Appl. Organomet. Chem.*, 2011, vol. 25, no. 3, p. 180.
4. Fukin, G.K., Baranov, E.V., Jelsch, C., et al., *J. Phys. Chem. A*, 2011, vol. 115, no. 29, p. 8271.
5. Fukin, G.K., Baranov, E.V., Poddel'sky, A.I., et al., *ChemPhysChem*, 2012, vol. 13, no. 17, p. 3773.
6. Ilyakina, E.V., Poddel'sky, A.I., Cherkasov, V.K., and Abakumov, G.A., *Mendeleev Commun.,* 2012, vol. 22, no. 4, p. 208.
7. Fedushkin, I.L., Moskalev, M.V., Lukoyanov, A.N., et al., *Chem.-Eur. J.*, 2012, vol. 18, no. 36, p. 11264.
8. Fedushkin, I.L., Nikipelov, A.S., and Lyssenko, K.A., *J. Am. Chem. Soc.*, 2010, vol. 132, no. 23, p. 7874.
9. Piskunov, A.V., Meshcheryakova, I.N., Fukin, G.K., et al., *Dalton Trans.*, 2013, vol. 42, no. 29, p. 10533.
10. Piskunov, A.V., Ershova, I.V., Fukin, G.K., and Shavyrin, A.S., *Inorg. Chem. Commun.*, 2013, vol. 38, no. 12, p. 127.
11. Piskunov, A.V., Chegerev, M.G., and Piskunova, M.S., *Izv. Akad. Nauk, Ser. Khim.*, 2014, no. 4, p. 912.
12. Kolyakina, E.V., Vaganova, L.B., Piskunov, A.V., et al., *Izv. Akad. Nauk, Ser. Khim.*, 2007, no. 7, p. 1314.
13. Kolyakina, E.V., Vaganova, L.B., Piskunov, A.V., et al., *Vysokomol. Soedin., Ser. A*, 2008, vol. 50, no. 2, p. 260.
14. Vaganova, L.B., Kolyakina, E.V., Lado, A.V., et al., *Vysokomol. Soedin., Ser. B*, 2009, vol. 51, p. 530.
15. Vaganova, L.B., Maleeva, A.V., Piskunov, A.V., and Grishin, D.F., *Zh. Prikl. Khim.*, 2011, vol. 84, no. 11, p. 1872.
16. Vaganova, L.B., Maleeva, A.V., Piskunov, A.V., and Grishin, D.F., *Izv. Akad. Nauk, Ser. Khim.*, 2011, no. 8, p. 1594.
17. Vaganova, L.B., Shchepalov, A.A., Meshcheryakova, I.N., et al., *Dokl. Ross. Akad. Nauk*, 2012, vol. 447, no. 6, p. 634.
18. Vaganova, L.B., Kaprinina, A.N., Meshcheryakova, I.N., et al., *Izv. Akad. Nauk, Ser. Khim.*, 2014, no. 3, p. 744.
19. Gordon, A. and Ford, R., *The Chemist's Companion: A Handbook of Practical Data, Techniques, and References*, New York: Wiley, 1972.
20. Sheldrick G.M., *SHELXTL. Version 6.12. Structure Determination Software Suite*, Madison (WI, USA): Bruker AXS, 2000.
21. Sheldrick G.M., *SADABS. Version2.01. Bruker/Siemens Area Detector Absorption Correction Program*, Madison (WI, USA): Bruker AXS, 1998.
22. Piskunov, A.V., Meshcheryakova, I.N., Baranov, E.V., et al., *Izv. Akad. Nauk, Ser. Khim.*, 2010, no. 2, p. 354.
23. Emsley, J., *The Elements*, Oxford: Oxford Univ., 1991, p. 256.
24. Batsanov, S.S., *Zh. Neorg. Khim.*, 1991, vol. 36, no. 12, p. 3015.
25. Zemlyansky, N.N., Borisova, I.V., Kuznetsova, M.G., et al., *Organometallics*, 2003, vol. 22, no. 8, p. 1675.
26. Zemlyanskii, N.N., Borisova, I.V., Nechaev, M.S., et al., *Izv. Akad. Nauk, Ser. Khim.*, 2004, no. 5, p. 939.
27. Razuvaev, G.A., Abakumov, G.A., Bayushkin, P.Ya., et al., *Izv. Akad. Nauk SSSR, Ser. Khim.*, 1985, p. 2098.

Translated by E. Yablonskaya